# Experimental Investigation on the Parameters Affecting Fuel Fretting Wear

Hyung-Kyu Kim*, Heung-Seok Kang, Kyung-Ho Yoon and Kee-Nam Song

Korea Atomic Energy Research Institute, 150 Dukjin-dong, Yusong-ku Taejon, 305-353 Korea

## ABSTRACT

Fretting wear of a fuel rod cladding tube of a pressurized water reactor is studied experimentally. Specially designed equipment for the present experiment is introduced. Experiments are conducted in air at room temperature. The intrinsic purpose of the present research is to derive a mechanical design technology to alleviate the fuel fretting wear. Cause of the fuel fretting is known to be the flow-induced vibration (FIV) in a reactor. However, it is necessary to consult a solid mechanical approach to solve the fretting problem by improving the spacer grid design. Present work utilizes the contact mechanical approach basically. Especially, the influence of the contact contour and the slip direction on fretting wear is brought into focus. To this end, spacer grid springs with concave, convex and flat contours are used for the specimens. Experiments with either axial or transverse slip direction are carried out. The slip range at which wear increases considerably (termed '*critical slip range*') is also concerned. For analyzing wear, wear depth on the tube is measured by a surface roughness tester and its volume is evaluated. As a result, a spring with concave contour is suggestible to restrain the fretting wear. Wear becomes more severe in the case of axial slip. The critical slip range is found around 80 ~ 100 $\mu$m.

## INTRODUCTION

To achieve a failure-resistant fuel, a remedy for fuel fretting has been pursued in the nuclear industry. The difficulty of preventing fuel fretting wear arises since cyclic contact stresses between spacer grid and fuel rod are inherent due to FIV. However, it may be addressed that a solid mechanical approach on the improvement of contact design can give the solution rather than the analysis of FIV. Wear is a phenomenon of particle removal from the contact surface due to cyclic shear stress on the contact. But to deal with the wear problem is not that simple. Even though there has been a lot of research on investigating, modeling and preventing fretting wear, it is still a difficult problem for designers and researchers to derive a general solution for wear. This is mainly because a lot of factors are related with the wear phenomenon. For instance, wear is affected by a combination of contacting materials, the environment, the loading conditions, the geometry of the contacting bodies, etc. Therefore, to find a solution for wear control even for specific conditions would also be meaningful. So to speak, to deal with the stress is one of the important methodologies to achieve a fretting failure resistant fuel.

In the fuel fretting problem, one of the considerations is to improve the spacer grid design, especially, the shape of the springs (or dimples). In this work, we confine ourselves to the spring only since the dimple can be regarded as a specific shape of spring. It is an application of contact mechanics, that is, the improvement of contact geometry by changing the spring shape can alleviate the contact stresses and their profile, which can restrain the fretting wear. The shape of the spring, especially the contour at the region of contact with the fuel rod, may be concave, flat or convex. On the other hand, when the fuel rods vibrate inside the spacer grids, the direction of rod motion must be arbitrary. But, we can decompose the shear force into the transverse and axial directions. The transverse shear (or slip) has been usually concerned. It occurs when a fuel rod moves in a plane perpendicular to the axis of the fuel assembly. However, the axial shear is also expected when the fuel rods deflect due to the FIV. The transverse and axial slips of the fuel rod inside the spacer grid are illustrated in Fig. 1.

Since the magnitude of slip is a major parameter of wear, to find a certain value of slip range from which wear becomes severe is also important to remedy the fuel fretting failure. This may be used for FIV control (if possible), spring

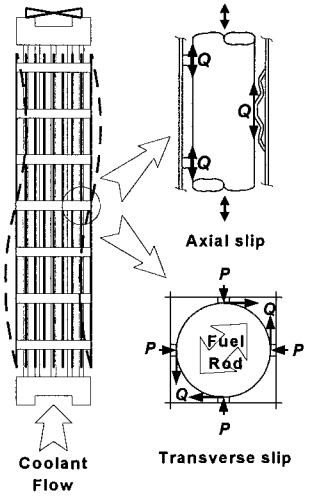


Fig. 1 Axial and transverse slip on the contact due to fuel rod vibration.

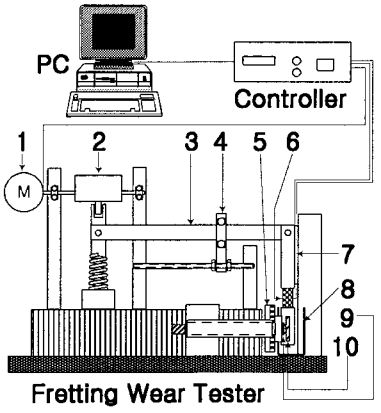


Fig. 2 Schematic diagram of fretting wear tester;
1: Servo-Motor, 2: Eccentric Cylinder, 3: Lever, 4: Movable Hinge, 5: Rotating Device, 6: Biaxial Loadcell, 7: LVDT, 8: Water Tank, 9: Stationary Specimen (Spring), 10: Oscillating Specimen (Tube).

force and shape, and number of contacts between spring and fuel rod. In the present work, the above concerns are dealt with experimentally. So we examine the influence of these parameters (i.e., spring shape, slip direction and range) on wear of specimen. The purpose of the present work is to obtain a basic view of the solution to remedy the fuel fretting failure by improving the design of the spacer grid and the relative motion between the spring and the fuel rod.

## EXPERIMENT

### Fretting Wear Tester

A fretting wear tester is specially designed for the present experiment. A schematic diagram of the tester is shown in Fig. 2. A DC servomotor is equipped and is connected to an eccentric cylinder (or cam). A roller, supported by a stiff spring, is in contact with the eccentric cylinder, to which a lever is connected. An assembly of small steel balls surrounds the lever, which can move along the axial direction of the lever by rotating an adjusting nut. The contacting point of the balls and the lever becomes a hinge. The other end of the lever is connected to the holder of oscillating specimen. In short, the tester uses a simple cam-lever mechanism, which changes a rotating motion to a reciprocating one. The motor speed is adjustable, so the test frequency can be changed.

Contacting normal force is exerted onto the oscillating specimen by translating the stationary specimen toward the oscillating one. As the stationary specimen presses the oscillating one up to a pre-determined normal force, a slip occurs between the two contacting specimens. The slip range (peak to valley) can be set at a certain value by adjusting the hinge location. It can be varied continuously without discrete steps. The slip range is measured by LVDT, which is attached to the holder of the oscillating specimen. The holders for the stationary and oscillating specimens are also specially designed. The fixture for the stationary specimen holder can rotate by up to 90° and the oscillating specimen can also be aligned perpendicularly by using a special specimen holder. This affords a various alignment of the contacting specimens. For example, it is useful when the slip direction needs to be changed arbitrarily.

The developed tester can measure the shear force, which is produced due to the friction between the two contacting specimens. A Biaxial load cell installed at the upper part of the oscillating specimen holder measures the normal and the frictional shear forces on the contact. The oscillation of the shear force and the slip are sinusoidal as the motor rotates. The parameters of fretting experiment, such as frequency, slip range, normal force, and shear force range and its mean value, are displayed and stored in the personal computer on a real time basis. On the other hand, a water tank, in which a heater and a

thermocouple are procured, is also equipped so that the fretting experiment can be conducted in water up to the boiling temperature.

**Specimen**

To simulate the fuel rod vibration in a fuel assembly, a tube of fuel cladding is used as an oscillating specimen. While, spacer grid strap of a cell size is used as a stationary specimen in the experiment. In total four different types of spring are used, as shown in Fig. 3. In Table 1, the characteristic of each spring is summarized independently. In short, the type of the spring specimen can be classified by its contour where the tube contacts. Springs A and B are intended to have a conformal contact with the circumferential surface of the tube specimen, while springs C and D have a non-conformal contact with it. The difference between A and B is the spring length and the end condition (i.e., both ends of spring A are fixed to the strap, but one end of spring B is free like a cantilever). The contour of spring C is convex so that a point contact is constituted between the tube and the spring. While, the contour of spring D is flat. Therefore, the contact length in Table 1 is the spring length for the springs A, B and D. For spring C, on the other hand, it is calculated from the contacting normal force and radius of spring by assuming Hertzian contact between the spring and the tube.

The tube specimen is cut to be 50 mm in length from the as-received cladding tube for fuel fabrication. The outer diameter and the thickness are 9.5 mm and 0.6 mm, respectively. The tube and the spring specimen are made of Zircaly-4. The mechanical properties and the chemical compositions of the material are listed in Table 2. All the specimens are carefully cleaned with acetone before conducting the experiment. Surface roughness tester reads the arithmetic average of the specimen roughness ($R_a$) before the experiment, which is 0.76 $\mu$m for the tube and 0.67 $\mu$m for the spring.

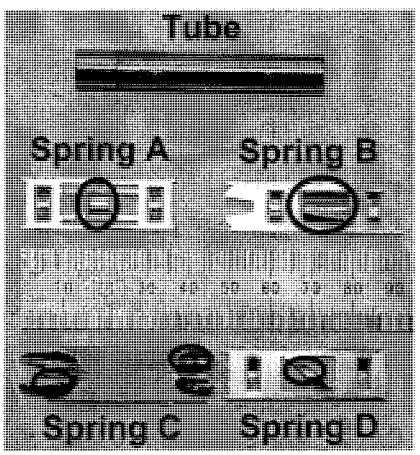


Fig. 3 Spring specimens (circle designates the spring which is in contact with tube specimen).

Table 1. Summary of the characteristic of spring specimen.

| Spring shape | Contact contour | End condition | Contact length intended | No. of contacts |
|---|---|---|---|---|
| A | Concave | Clamped at both ends | 5.0 mm | 1 |
| B | Concave | Cantilever | 11.1 mm | 1 |
| C | Convex | appr. Cantilever | 0.274 mm* | 2 |
| D | Flat | Clamped at both ends | 2.5 mm | 1 |

*: Evaluated assuming Hertzian contact.

Table 2. Mechanical and Chemical properties of Zircaloy-4..

| Mechanical properties (at room temperature) | | | | |
|---|---|---|---|---|
| Tensile strength | Yield strength (0.2% offset) | Elongation in 2″ | Elastic Modulus | Poisson's Ratio |
| 470 MPa | 315 MPa | 31% | 136.6 GPa | 0.294 |

| Chemical composition (wt. %) | | | | | | |
|---|---|---|---|---|---|---|
| Sn | Fe | Cr | O | C | Si | Zr |
| 1.28 | 0.22 | 0.12 | 0.114 | 0.013 | 0.010 | remained |

**Procedure**

Two kinds of experiment are conducted in this work. For the first category (termed as 'Category 1'), the effect of the spring type and the oscillating (slip) direction on wear are investigated. In this experiment, contacting normal force is set 20 ± 1 N. Range of relative motion between the spring and the tube (slip range) is set 14 ± 1 $\mu$m. The tube specimen oscillates with 30 Hz since it is regarded to be near the first natural frequency of a fuel rod. Each experiment is carried out until the number of reversals of the tube oscillation reaches 300,000.

The specimen alignment for axial and transverse slip is depicted in Fig. 4. In axial slip, tube specimen oscillates in axial direction and spring specimen is aligned also in axial direction. However, for the experiment of transverse slip, the

spring is rotated by 90° and tube specimen is inserted into the tube holder in a perpendicular direction to the holder axis. This is because the direction of oscillation is fixed vertically. Experiments of both axial and transverse slip are carried out for each type of the spring.

As for the second category (termed as 'Category 2'), critical slip range for severe wear is investigated for spring D. Here, the critical slip range is defined as a slip range between the spring and the tube from which the wear becomes much more severe. In this experiment, normal force is set 30 N and the number of cycle is fixed as 100,000. The slip range is varied as 10, 30, 50, 80, 100, 150 and 200 $\mu$m. Both axial and transverse slip directions are also applied for this experiment. Additionally, a similar experiment with normal force being 50 N is conducted to see the effect of normal force. All of the present experiments are conducted in air at room temperature.

When each experiment is finished, the wear scar on the contact surfaces of both tube and spring are observed. Detail measurement, investigation and analysis are done for the wear on the tube. The worn surface is measured in two ways; firstly the overall worn area is measured by a measuring microscope, then secondly, the contour of the worn area is traced by a stylus of the surface roughness tester. During the stylus movement along the axial direction of a tube, wear contour is obtained. As the movement is repeated in a transverse direction with a pre-determined fine distance, a whole 3-dimensional shape of wear can be reproduced. The maximum depth and volume of the wear are obtained from this data.

To evaluate the wear volume is often necessary to analyze the wear phenomenon, especially for wear modeling. In this work, wear volume is evaluated by using a specially developed program. The algorithm of it is based on a signal processing technique such as Fast Fourier Transform and Windowing [1]. $R_a$ value of the tube specimen (= 0.76 $\mu$m) is used for the baseline of the volume integration. The program is very much useful when the wear is locally distributed on the contact surface and its shape is arbitrary, as are found in the present experiment.

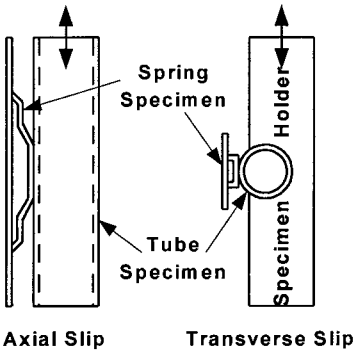


Fig. 4 Alignment of specimens for the experiment of axial and transverse slip.

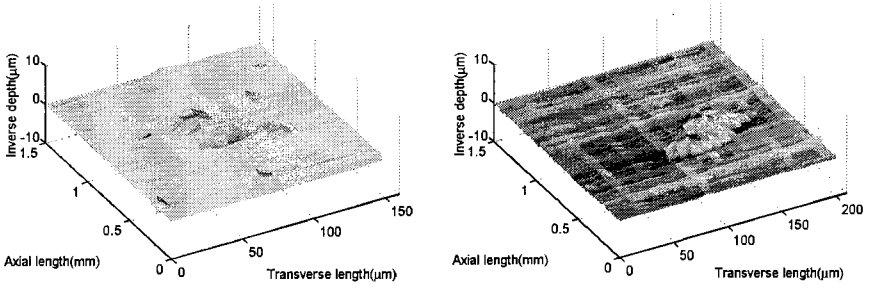


Fig. 5 Worn surface view in the experiment of axial slip; left: wear by spring A, right: wear by spring B. Wear is displayed as protrusion. Left view shows wider distribution of wear scar.

## RESULTS AND DISCUSSION

### Category 1

In wear, the slip condition on the contact surface can be classified as partial and gross slip. The slip range and the normal force influence the condition of slip. In gross slip, the whole contact area slips so that the wear occurs on the whole area. To the contrary, part of contact area (contact boundary, in general) slips in partial slip. So the wear becomes much more severe in gross slip than in partial slip. It is regarded that the slip range (14 $\mu$m nominal) and the normal force (20 N nominal) of the present experiment are within the range of gross slip according to the fretting map [2]. However, it is difficult to say that the gross slip is formed in the experiment since the wear scar is found localized within the contact area as shown typically in Fig. 5. It is observed that the length (in axial direction) of the localized worn area is always much shorter than the spring length and the location is not coincident with the contact boundary. So, it cannot be said that the partial slip condition

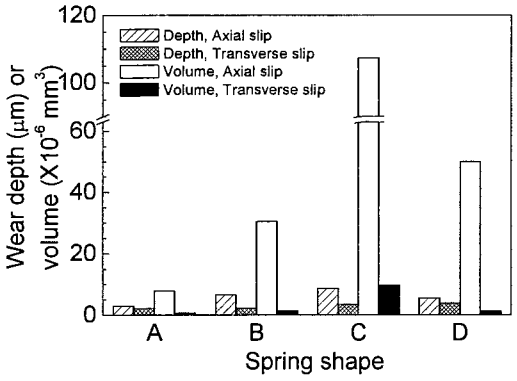


Fig. 6 Comparison of wear depth and volume with respect to slip direction and spring shape.

prevails presently either.

Within a wear scar, the trace shows 'W' shape contour. This means that the outer region of a wear is deeper than the inner (central) region in all cases. The difficulty of determining the slip condition may be attributed to the geometry of the contacting bodies. The fretting map consulted [2] arranged the wear results in the case of a ball contact on a square block, i.e. a well-controlled Hertzian contact. In the present experiment, however, the globally flat contact ends of both spring and tube may not guarantee that the full length of spring contacts with tube. Alignment problems may also cause localized wear. If the axes of spring and tube are not parallel, real contact occurs on a part of spring length. Nevertheless, the present experiment is thought meaningful since it can accommodate the real situation of fuel rod insertion into the spacer grid.

Resultantly, the wear depth and volume investigated from each spring and slip direction are averaged and depicted in Fig. 6. The maximum depth of wear is found smaller in the case of contact with springs A and B than springs C and D, regardless of the slip direction (except the case of axial slip with spring B, it is slightly deeper than the case with spring D). But the difference is not discriminating. On the other hand, the evaluated wear volume apparently reveals the difference further. The wear volume caused by the spring with concave contour (springs A and B) is less than that caused by the convex (spring C) and the flat (spring D) springs, which was expected before conducting the experiment. If the spring has a concave contour, the contact *width* can be larger which results in the wider distribution of contact stresses and less wear.

When we compare the wear by springs A and B from Fig. 6, the wear by spring A is less than that by spring B. It is expected at the outset that the longer spring (spring B in this case) causes less wear since the contact stress can be distributed further more. However, the result is contradictory to our expectation. We attribute this contradiction to the different structural shape between springs A and B. As stated in Fig. 3 and Table 1, spring B has a free end at one side, while spring A is fixed at both ends. Therefore, in spring B, the location of contact on the spring can be moved as the contacting normal force is applied since it is *bent* rather than *displaced*. Simultaneously, a rotation around the transverse (horizontal) axis may occur when spring B is bent. This can reduce the actual contact length considerably, especially when the spring has a concave contour. The end condition of spring A (fixed at both ends) can alleviate this problem. This is verified from the observation of the worn area on the tube (see Fig. 5). So to speak, the worn region is found more widely distributed in the case of contact with spring A than spring B.

An interesting result is that the wear volume caused by contact with spring C (convex contour) is considerably greater than the others. This can be explained by the smallest contact area among the spring types and the reduced normal force due to the number of contact. High stress concentration is produced on the contact surface due to the smallest contact area. Since the number of contact between spring C and tube is two rather than one, unlikely to the other springs, the normal force for one contact region is approximately half (i.e., $\simeq$ 10 N) of the applied force (moment is neglected here). This may constitute a gross slip condition further. In the case of the contact with flat spring (spring D), wear volume is much less that the case with spring C but greater than the case with concave springs. Again, the contact length and width, and the number of

contact (one in this case) explain this.

From the above results, wear in the case of axial slip is much more severe than that in the case of transverse slip. This implies that the tube oscillation in the axial direction needs to be controlled. Additionally, it can be said from the present findings that it is not sufficiently true to concern primarily the transverse direction in dealing with the fuel fretting problem. For instance, fuel fretting failure previously experienced as shown in Fig. 7 can be explained if the axial slip is taken into account. The length of the wear area in Fig. 7 reveals longer than the spring used while the width of it is almost the same as that. When the fuel vibrated, relative motion in axial direction seemed to play the major role in wear for this case. An analytical method has been expressed previously by the first author for sequential axial and transverse slip with a possible scenario of axial slip on the contact between spring and cladding tube [3].

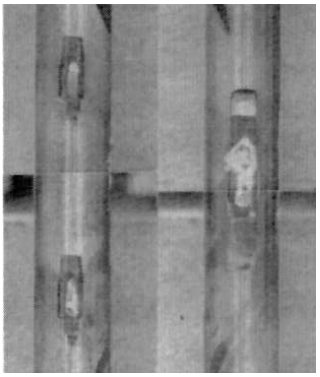

Fig. 7 Typical view of fretting wear on the fuel rod surface.

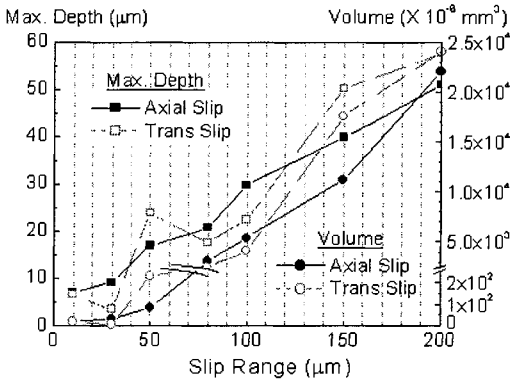


Fig. 8 Variation of maximum depth and volume of wear by spring D (normal force: 30 N).

**Category 2**

As is widely known, the intrinsic cause of fuel fretting is flow induced vibration. Therefore, the fretting phenomenon of fuel cannot be removed completely in the reactor. In the mechanical design point of view, the factors such as shape, structure, force and alignment control of the spacer grid spring can alleviate the fretting failure by detailed interpretation and analysis of Category 1 results. On the other hand, these factors can also affect the slip range itself when the flow condition is the same. Since wear is very much influenced by slip range, to find a certain range below which wear is restrained (if it exists) may be very important. The purpose of the Category 2 experiment is to investigate the existence of such a slip range and the value.

Spring D is used in this experiment since it has the most general shape (i.e., flat contour) in the commercially available fuel. The result is given in Fig. 8. In short, it is apparently found that a critical slip range exists and the value is 80 $\mu$m in the present case. In Fig. 8, the maximum wear depth increases as the slip range increases. There is no considerable jump of the depth in the case of axial slip. In transverse direction, however, the depth at the slip range of 30 $\mu$m is smaller than that at 10 $\mu$m and the depth at 50 $\mu$m is larger than that at 80 and 100 $\mu$m. This may be due to misalignment of the specimens since to align the tube specimen in parallel to the spring is comparatively difficult in the experiment of transverse slip. Nevertheless, it cannot change the considerable volume increase at 80 $\mu$m.

The critical slip range of 80 $\mu$m can be apparently found if the contact surface is examined. Fig. 9 shows the worn surfaces on the tube in the case of the ranges being 50, 80 and 100 $\mu$m. Both results of axial and transverse slip are given. The view of 10 and 30 $\mu$m is similar to that of 50 $\mu$m, and the view over 100 $\mu$m is similar to 100 $\mu$m. So those are not included in Fig. 9. Up to 50 $\mu$m, localized wear is found at the location where the outer part of spring contacts. A whole contact area is found worn from the slip range of 80 $\mu$m. This phenomenon is common to both results of axial and transverse slip. From the definition of partial and gross slip, the boundary between them may locate within the range 50 ~ 80 $\mu$m when the normal

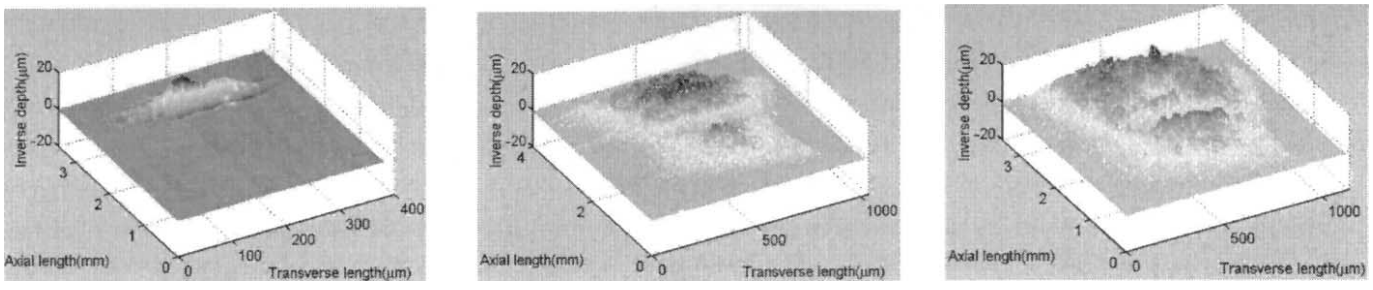


at 50 $\mu$m at 80 $\mu$m at 100 $\mu$m

(a) Axial slip

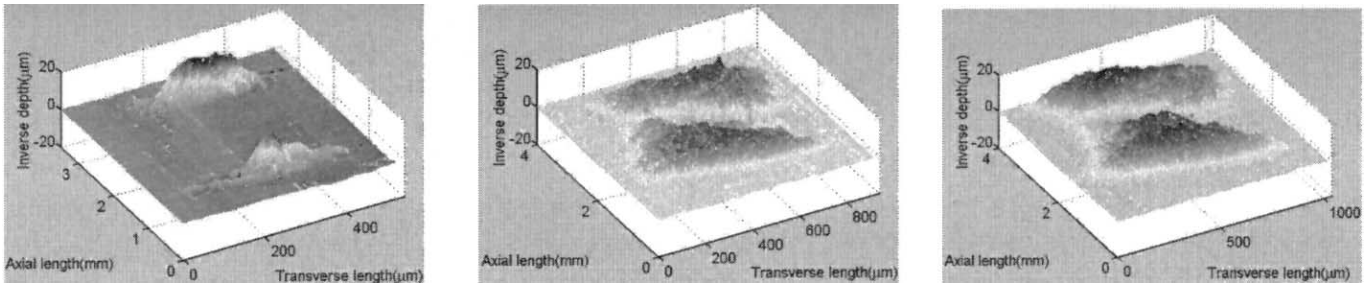


at 50 $\mu$m at 80 $\mu$m at 100 $\mu$m

(b) Transverse slip

Fig. 9 Wear evolution as slip range increases (at normal force being 30 N, spring D is used).

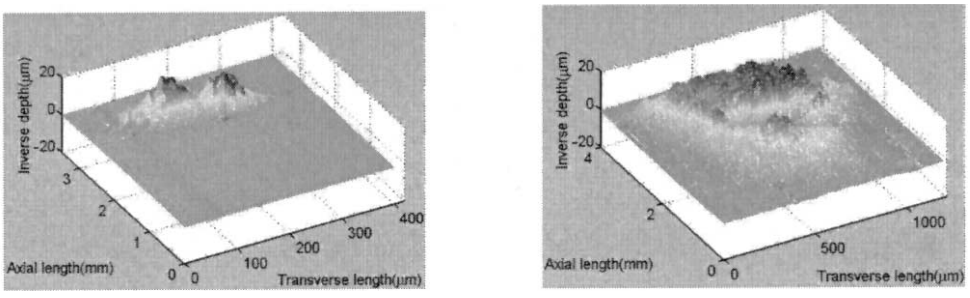


at 80 $\mu$m at 100 $\mu$m

Fig. 10 Wear evolution as slip range increases (at normal force being 50 N, result of axial slip with spring D). The evaluated wear volumes at 80 and 100 $\mu$m are $1.99X10^{-4}$ and $5.06X10^{-3}$ $mm^3$, respectively.

force is 30 N. It is much higher than that shown in the fretting map [2], which read about 14 $\mu$m. This can also be attributed to the geometrical difference as stated in the previous subsection (Category 1).

From a similar experiment of critical slip range, it has been said that the critical range is dependent on the material but was found within the range of 50 ~ 100 $\mu$m [4]. In the case of tube to tube (made of Zircaloy-4) contact, it was also found around 100 $\mu$m [5]. In order to confirm this, an extra experiment is conducted with the normal force of 50 N and the slip ranges of 80 and 100 $\mu$m. The reason of choosing these values is that, if normal force is larger, the slip range of the boundary between partial and gross slip should also increase accordingly. As a result, the critical slip range is shifted to 100 $\mu$m from 80 $\mu$m as shown in Fig. 10. Therefore, it may be said that gross slip begins from the critical slip range, so it varies with the

normal force. However, the dependence of the critical range on the shape of spring is still unknown, which will be carried out. It is highly necessary to find the critical slip range for a specific spring, since it can give valuable design data for restraining the fuel fretting failure.

## CONCLUDING REMARKS

The final target of the present work is to establish mechanical design technology to restrain fuel fretting failure. To this end, the specific study here is to investigate the parameters experimentally that affect the fretting phenomenon. As for the parameters, the structural shape including contour, the slip direction and the critical slip range are concerned. With using the specially designed wear tester and algorithm for volume evaluation, we find the following results; first, the relative motion in the axial direction should be concerned since the wear by axial slip is always found severer than that by transverse slip. As the second remark, the spring of concave contour is comparatively suggestible because it causes less wear, in general, than the spring of convex or flat contour. On the other hand, it is found better for restraining fretting wear if the spring is fixed at both ends rather than free at either end, since the former can provide more stable contact with the cladding tube when the spring is compressed. The critical slip range for the spring of flat contour is 80 $\mu$m and 100 $\mu$m when normal force is 30 N and 50 N, respectively. Presently, the critical slip range is thought to determine the boundary of partial and gross slip conditions. It is highly required to control the vibration amplitude of fuel rod to be less than that causes the critical slip range to mitigate fuel fretting problem.

## ACKNOWLEDGEMENT

This project has been carried out under the Nuclear R&D Program by Ministry of Science and Technology of Korea.

## REFERENCES

1. Kim, -H.K. and Kim, -S.J., "Development of algorithm for wear volume evaluation using surface profile analysis," *J. Korean Society of Tribologists and Lubrication Engineers*, 2000, submitted for publication.
2. Fouvry, S., Kapsa, P. and Vincent, L., "Quantification of fretting damage," *Wear*, Vol. 200, 1996, pp. 186-205.
3. Kim, -H.K., "Mechanical analysis of fuel fretting problem," *Nuclear Engineering and Design*, Vol. 192, 1999, pp. 81-93.
4. Iwabuchi, A., "The effect of slip amplitude and load in fretting wear," *J. Japan Society of Mechanical Engineers*, Vol.44, 1978, pp. 692-699.
5. Cho, -K.H., Kim, -T.H. and Kim, -S.S., "Fretting wear characteristics of Zircaloy-4 tube," *Wear*, Vol. 219, 1998, pp. 3-7.